

Utilization of BLDC motor in electrical vehicles

Abstract. The paper presents results of works concerning utilization of BLDC motor in electrical vehicles in mechatronic system composed of battery of accumulators, power electronic converter and three-phase winding brushless direct current motor (BLDCM) with permanent magnets. Comparison of simulation and registered steady states of electrical and mechanical quantities: voltages, currents, mechanical torque and speed of the rotor for the mechatronic drive system in a test-bed especially designed and constructed for the experiment have been carried out.

Streszczenie. W niniejszym artykule przedstawiono wyniki badań dotyczące wykorzystania silnika BLDC w pojazdach z napędem elektrycznym w układzie mechatronicznym złożonym z baterii akumulatorów, przekształtnika oraz bezszczotkowego silnika prądu stałego (BLDCM) z magnesami trwałymi z trójfazowym użwojeniem. Porównano wyniki badań wielkości elektrycznych i mechanicznych: napięć, prądów i momentu na wale przy ustalonej prędkości obrotowej dla układu mechatronicznego otrzymane na drodze symulacyjnej oraz eksperymentalnej w stanowisku badawczym specjalnie zaprojektowanym do przeprowadzania badań. (Wykorzystanie silnika BLDC w pojazdach z napędem elektrycznym)

Słowa kluczowe: BLDCM, układ mechatroniczny, badania symulacyjne i eksperymentalne, stanowisko badawcze.

Keywords: BLDCM, mechatronic system, simulation and experimental investigations, test-bed.

Introduction

Owing to a small inertia moment, when compared with direct current commutator motors, as well as the vectorial way of control, brushless DC motors (BLDCM) with permanent magnets demonstrate perfect regulating and dynamic properties. The motors have got a number of advantages: simple construction and also simple control system, the lack of mechanical commutator, high efficiency, good dynamic properties, high density of power, low turns and high value of torque. Those motors are widely applied to servomotors of industrial robots and machine tools, precision instruments, computer equipment as well as driving motors of different types of vehicles [1 - 6].

Moreover, they are also used as electric energy generators in autonomous devices [6]. In the paper in simulations and experiment three-phase winding brushless DC motor with permanent magnets was used rated data were as follows: nominal power $P_N = 125W$, nominal current $I_N = 8A$, nominal voltage $U_N = 24V$, rotational speed $\Omega_N = 120$ rpm, nominal torque $T_N = 10Nm$, break-down torque, $T_K = 40Nm$, three-phase star-connected winding, stator diameter 135mm, air-gap 1 mm, Vacodynam 353 permanent magnets – 3mm in thickness. The total mass of the motor was 5.5 kg.

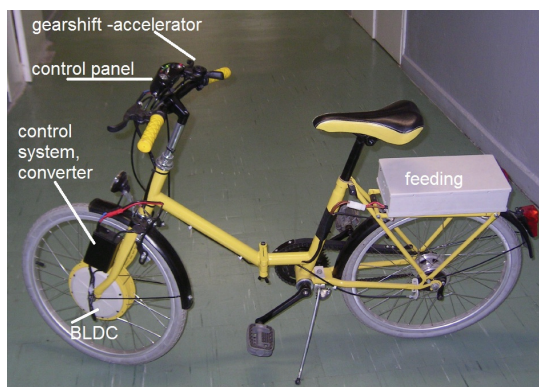


Fig. 1. General view of the electric bike

Utilization into urban traffic relatively cheap light vehicles with power electronic drive could reduction of the emission of local fumes coming from combustion vehicles. Moreover, applying of the unconventional sources to electric vehicles directly driven, like high efficient batteries are looked very promisingly, and leads to the reduction of global emission of the fumes. The main difficulty of vehicles with electric motor rapid introduction of is due to the limitations in

technology of battery production. Thanks to modern technology of electric motors construction, e.g. brushless direct current motors with permanent magnets (BLDCM with PM), as well as the improvements of lead-acid batteries, contemporary electric vehicles compete with conventional drives very well in respect of: the driving speed, the maximum speed, obtained accelerations, grade ability, etc [1- 6].

Fig. 1 and Fig. 2 show general view of the electric bike and a cross section of the BLDCM that in the paper was used in simulations and experiment.

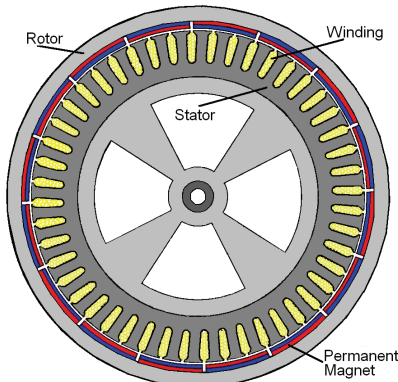


Fig. 2. Cross section of the BLDCM

BLDC motor drive system

One of the most important components of light electric vehicles equipped with DC motors with permanent magnets are batteries. They serve not only to supply energy in steady and dynamic BLDCM engine but also ensure the functioning of all electrical receivers such as electronic control systems and bicycle lights. The battery as one of the elements in the drive chain system must be efficient as long as possible. In each battery there are permanent and irreversible changes in the chemical structure of the active mass, which is a natural and inevitable phenomenon. Nevertheless, each battery life can be greatly extended. The longest-efficient batteries are those which are maintained close to full charge, which when applied to electric vehicles and frequent driving seems to be an unattainable ideal. Therefore, batteries operated in such a way must be recharged as often as possible. The main component leading to increase the bike travelling distance and extend the battery working

time is the impulse electronic circuit of transferring the energy coming from induced electromotive forces e_A , e_B , e_C in BLDC motor armature windings shown in the cross section of the BLDCM in Fig. 1. Brushless DC motors with permanent magnets, thanks to the presence of an external torque can also work as generators. The effective value of induced voltage for harmonic basis in the individual windings can be described by the relation

$$(1) \quad E = c \Omega \Phi n_1 k_{u1}$$

where: n_1 , k_{u1} – respectively the number of serial windings and a winding factor of one 3-phase motor winding, Φ - flux, Ω – rotational speed, c - constant.

In DC motors with permanent magnets, induced voltage value practically depends only on torque engine speed (frequency). Waveforms of induced electromotive forces e_A , e_B , e_C for speed $\Omega = 20$ rpm and 280 rpm in three-band windings in a tested BLDC star-oriented motor tested with the following rated data: $P_N=125W$, $U_N=24V$, $\Omega_N = 120\text{rpm}$ have been shown in Fig. 3

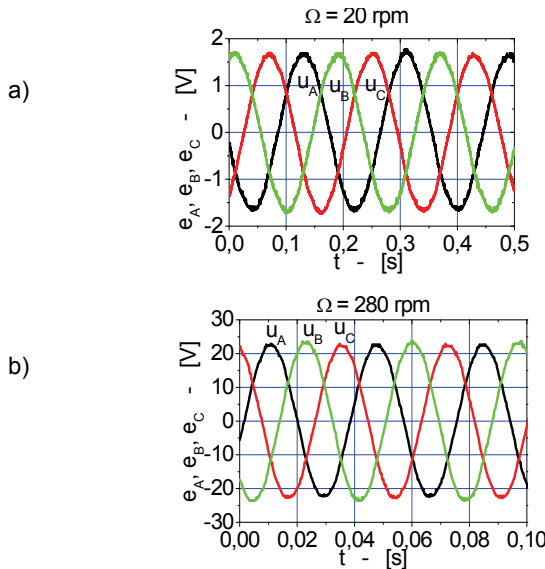


Fig. 3. Waveforms of induced electromotive forces e_A , e_B , e_C for Ω equal to: a) 20 rpm, b) 280 rpm

Table 1 gives the values of electric bike velocity Ω and amplitude of induced voltages E_m in the BLDCM vs rotational speed.

Table 1. Values of electric bike velocity and amplitude of induced voltages in the BLDCM vs rotational speed

Ω [rpm]	Electric Bike Velocity [km/h]	E_m [V]
20	1.85	1.69
40	3.90	3.38
80	7.80	6.76
140	13.60	11.84
200	19.50	16.89
280	25.90	23.65

In Fig. 4 the electric bike velocity (Fig. 1, Tab. 1) vs rotational speed was shown.

From the presented waveforms of induced voltages can be seen that for example the maximum instantaneous values for these voltages 23.65V, even for BLDC motor speed 280 rpm (and the corresponding riding speed 25.9 km/h) are smaller than the power supply voltage of two batteries connected in series. Therefore, frequent recharging of batteries in electric vehicles equipped with BLDC motors can

be realized by means of a frequency converter that is a pulse energy conversion system, which in the particular application to bicycles with electric drive system was realized as AC/DC converter increasing the voltage [5]. Currents flowing in the motor windings due to induced voltages after a suitable transformation can be used to recharge the batteries.

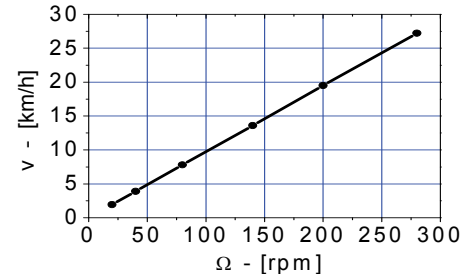


Fig. 4. The electric bike velocity vs rotational speed of BLDCM

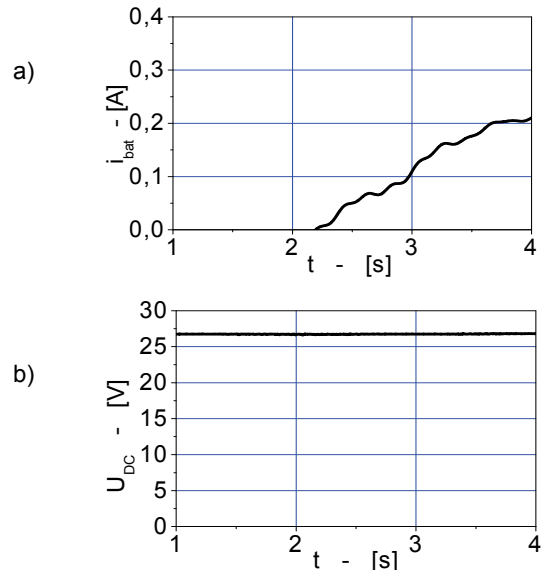


Fig. 5. Waveforms of a) current charging two accumulators connected in series, b) voltage on the two batteries connected in series

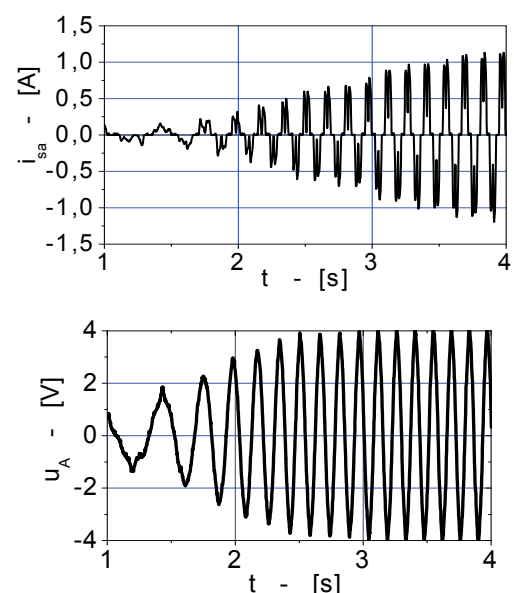


Fig. 6. Waveforms of a) armature current in phase A, b) phase voltage during giving back energy into the batteries coming from induced voltages in one of the BLDC motor windings

Development of a system for pulse charging of not a very complex and simple design in a electric drive of lightweight vehicles with BLDC motor has been presented in [5]. This system allows for frequent recharging the battery consisting of two batteries of 12 V, 7Ah connected in series, made in gel technology (electrolyte is trapped in a gel) marked as SLA (Sealed Lead-Acid - sealed lead-acid batteries). The battery is charging during the generator braking state of BLDC motor working, which is realised by the switched-off control system of the engine to the motor operation (disconnected microcontroller of Allegro Microsystems, Inc. company. type - 3933), and built, switched-on pulse energy system [5]. Recorded waveforms of current charging two accumulators connected in series i_{bat} and voltage on the two batteries connected in series U_{DC} has been shown in Fig. 5, while the armature current i_{sa} in phase A and phase voltage u_A during giving back energy into the batteries coming from induced voltages in one of the BLDC motor windings has been shown in Fig. 6.

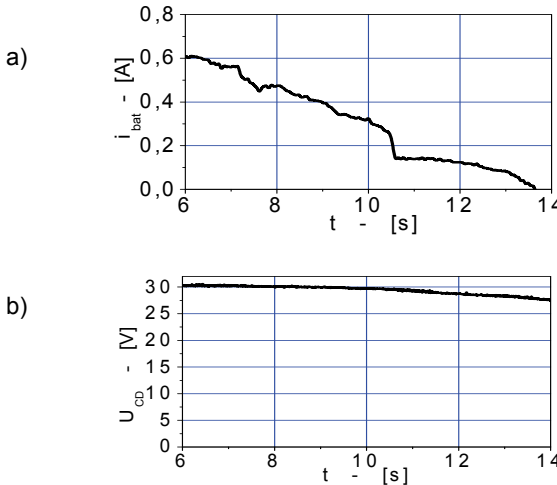


Fig. 7. Waveforms of a) current charging two accumulators connected in series, b) voltage on the two batteries connected in series during acceleration and changes in pulse width modulation (from the maximum to the 0)

In Fig. 7 were shown waveforms of current charging two accumulators connected in series and voltage on the accumulators during acceleration and changes in pulse width modulation (from the duty cycles 100% to the 0%) of the control system converter transistors (Fig. 1) to the rotational speed of 180 rpm. The initial rotational speed was 65 rpm (when the maximum current charging was set). In Fig. 7 were shown registered transients of armature current in phase A and phase voltage U_A .

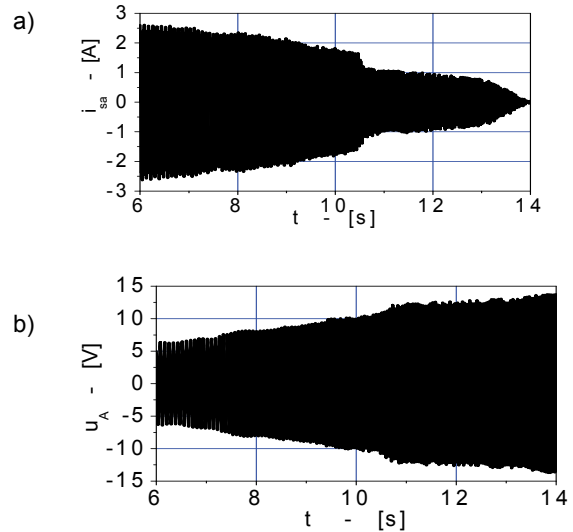


Fig. 8. Waveforms of a) armature current in phase A, b) phase voltage during acceleration and changes in pulse width modulation (from the maximum to the 0)

Fig. 9 shows a simplified equivalent electrical network of the control system converter (Fig. 1) for the brushless DC motor with permanent magnet used for feeding and controlling of the electric bike.

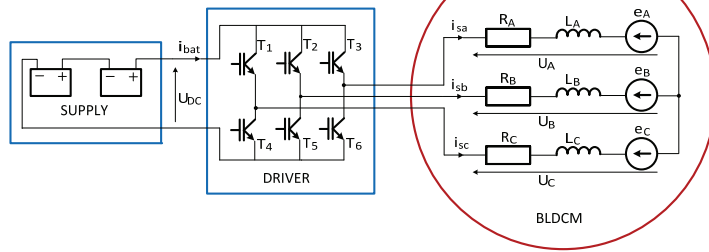


Fig. 9. Simplified equivalent electrical network for brushless DC motor with permanent magnet for feeding and controlling

The system shown in Fig. 9 is described with the following voltage equations:

$$(2) \quad \begin{bmatrix} u_A \\ u_B \\ u_C \end{bmatrix} = \begin{bmatrix} R_A & 0 & 0 \\ 0 & R_B & 0 \\ 0 & 0 & R_C \end{bmatrix} \begin{bmatrix} i_{sa} \\ i_{sb} \\ i_{sc} \end{bmatrix} + \frac{d}{dt} \begin{bmatrix} L_A & 0 & 0 \\ 0 & L_B & 0 \\ 0 & 0 & L_C \end{bmatrix} \begin{bmatrix} i_{sa} \\ i_{sb} \\ i_{sc} \end{bmatrix} + \begin{bmatrix} e_A \\ e_B \\ e_C \end{bmatrix},$$

where: $\begin{bmatrix} e_A \\ e_B \\ e_C \end{bmatrix} = K_b \Omega \begin{bmatrix} \sin p\varphi \\ \sin(p\varphi - \frac{2}{3}\pi) \\ \sin(p\varphi - \frac{4}{3}\pi) \end{bmatrix}$ – denote vector of induced electromotive forces in individual phase-winding, R_A, R_B, R_C

– denote resistance of one-phase armature winding, L_A, L_B, L_C – denote inductance of one-phase armature winding, p – denotes the number of pole pairs, φ – the angle between the axis of resultant flow of armature winding and the permanent magnets field, Ω – mechanical angular speed, K_b – const.

The mechanical system of the electric drive can be written as the following motion equation:

$$(3) \quad J \frac{d\Omega}{dt} = T_e - T_L - D\Omega$$

where: $T_e = \frac{e_A i_{sa}}{\Omega} + \frac{e_B i_{sb}}{\Omega} + \frac{e_C i_{sc}}{\Omega}$ – is electromagnetic torque, J – moment of inertia, T_L – load torque, D – damping friction coefficient.

BLDCM drive system used in simulations

Based on the voltage (2) and the motion (3) equations in the paper the mathematical model has been elaborated in Matlab/Simulink pack with taking into account SimPowerSystem toolbox. Blok diagram of the BLDC motor drive system corresponds to the equations (2) and (3) used in simulations is shown on the Fig. 9. PMSM motor model was used for simulation purposes which was located in SimPowerSystems Toolbox of Matlab/Simulink package. Shown in Fig. 9 BLDC motor model with PM for simulation purposes was equipped with the following elements:

- Two blocks *Decoder* and *Gates* performing control of power transistors of an inverter in a function of rotor position,
- BLDC motor block based on PMSM motor block,
- output part which enables the observation of selected output signals.

Fig. 10 shows a simplified equivalent electrical network of the control system converter (Fig. 1) for the brushless DC motor with permanent magnet used for feeding and controlling of the electric bike.

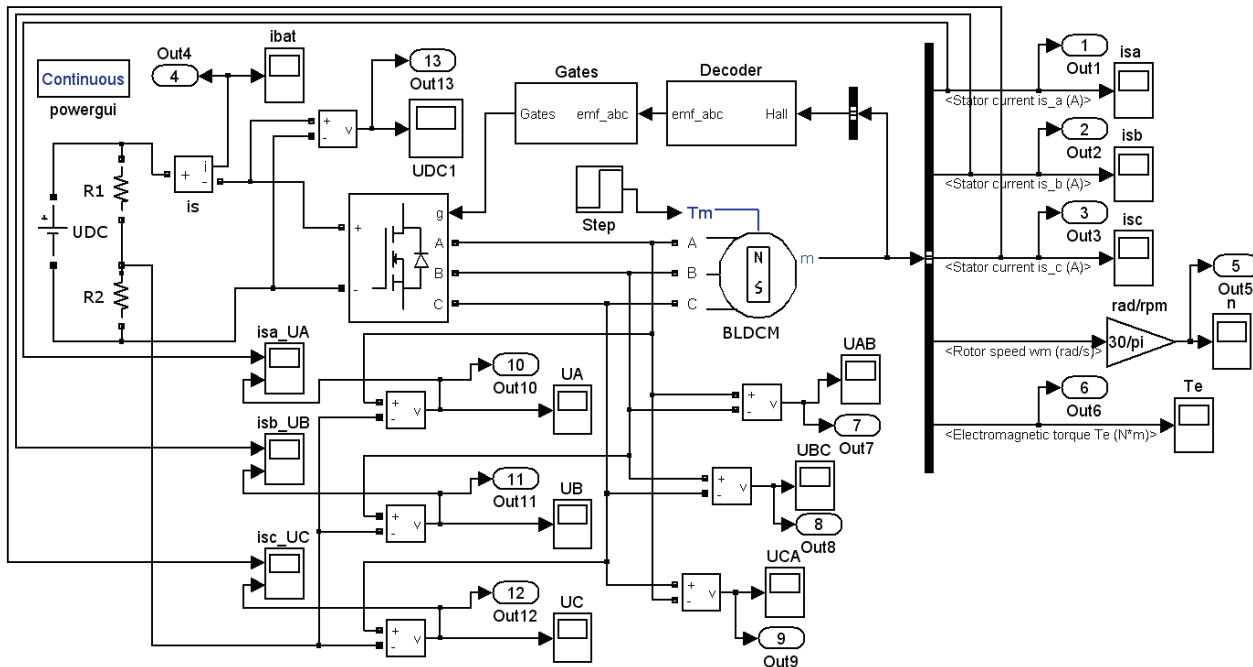


Fig. 10. Block diagram of the BLDC motor drive system used in simulations

An essential part of the model in Fig. 10 is a BLDC motor. The BLDC motor block is available in the Simulink program in SimPowerSystems toolbox. BLDC motor block has four inputs and one output. The inputs labelled *A*, *B*, *C* are the ends of the stator windings and to the terminal marked with *T_m* has been connected a Torque of mechanical load. The end marked with the letter *m* is the output of which via Bus Selector block can be led out following output signals:

- *i_{sa}*, *i_{sb}*, *i_{sc}* - armature currents flowing in stator windings,
- *wm* - rotor speed and angular position,
- *T_e* - electromagnetic torque.

In PMSM block, based on which BLDC motor model was built, the following parameters are defined

In *Configuration*, *Back EMF waveform tab* - determines the shape of the voltage i.e. sinusoidal or trapezoidal rotation (in this article has been selected the sinusoidal shape according to the recorded induced voltage diagrams in Fig. 3). *Mechanical input*, specifies the mechanical load torque (constant or time-dependent angular velocity (for this article has been chosen constant torque load), while the *Preset model*, enables to select one of sixteen PMSM motor models for which parameters have already been identified by Mathworks company, the creator of Matlab program. Selecting *No*, you can enter any motor parameters in the *Parameters tab*.

In *Parameters tab* the following BLDC motor parameters are introduced: phase stator winding resistance, stator windings inductance. If you have chosen a model with a sinusoidal voltage shape of the rotation then it is necessary to give inductance in *d* and *q* axis. However, if a model of the

trapezoidal shape of the rotation power has been selected, then you must specify the inductance of stator winding phase, in *Specify window* one of three parameters is determined:

- [Vs] magnetic flux caused by the action of permanent magnets or,
- [V_peak/rpm] constant voltage which determines maximum value of induced voltage per revolution, or,
- [Nm/A_peak] constant torque.

Moreover, in the *Parameters tab* are given the moment of inertia, viscous friction coefficient and the number of pole pairs as well as the initial conditions for the angular velocity of the motor, the rotor position and currents in the *a* and *b* windings bands.

Simulation studies were conducted by omitting viscous friction.

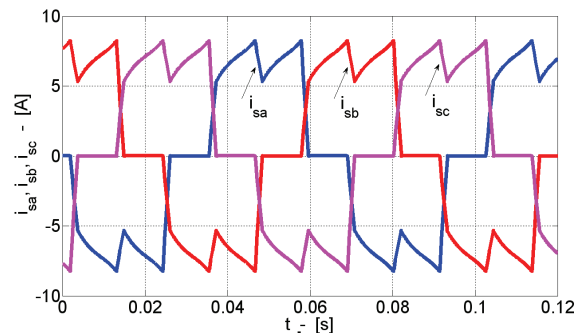


Fig. 11. Steady-state waveforms of armature currents

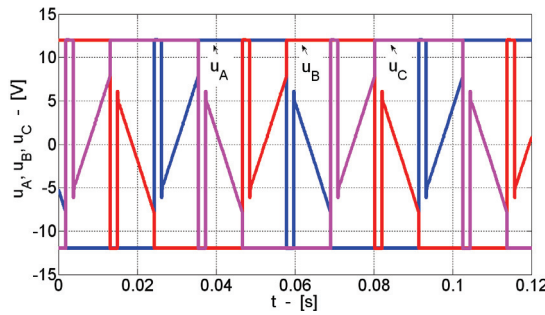


Fig. 12. Steady-state waveforms of phase voltages
a)

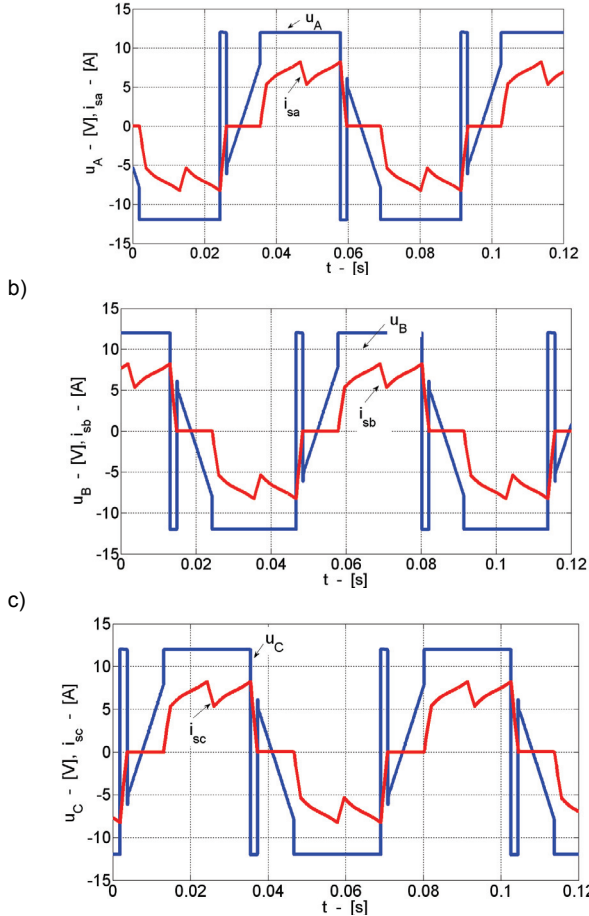


Fig. 13. Steady-state waveforms of phase voltages and currents a)
b) in phase B, a) in phase C

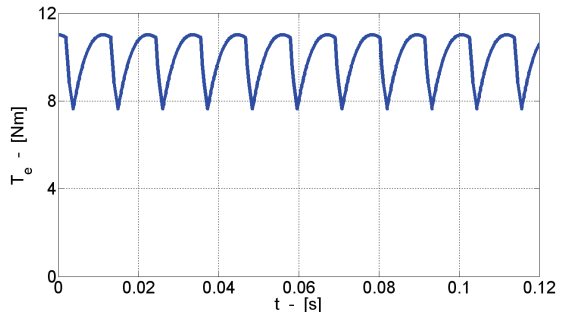


Fig 14. Waveform of the electromagnetic torque

Simulation studies in Matlab/Simulink of the Steady-state waveforms of armature currents (Fig. 11), phase voltages (Fig. 12), phase voltages (the blue waveforms) and currents (the red waveforms) in phase A, in phase B and in phase C (Fig. 13) and electromagnetic torque (Fig. 14) of the BLDC motor rated data $P_N=125W$, $U_N=24V$, $n_N=120\text{rpm}$ have been conducted.

Experimental verification

Fig. 15 shows a general view of the measurement set where voltages, currents, torque and rotational speed where recorded.



Fig. 15. General view of the measurement set for investigations of the brushless direct current motor

In Fig. 16 the block diagram of the measurement set (shown in Fig. 15) is presented.

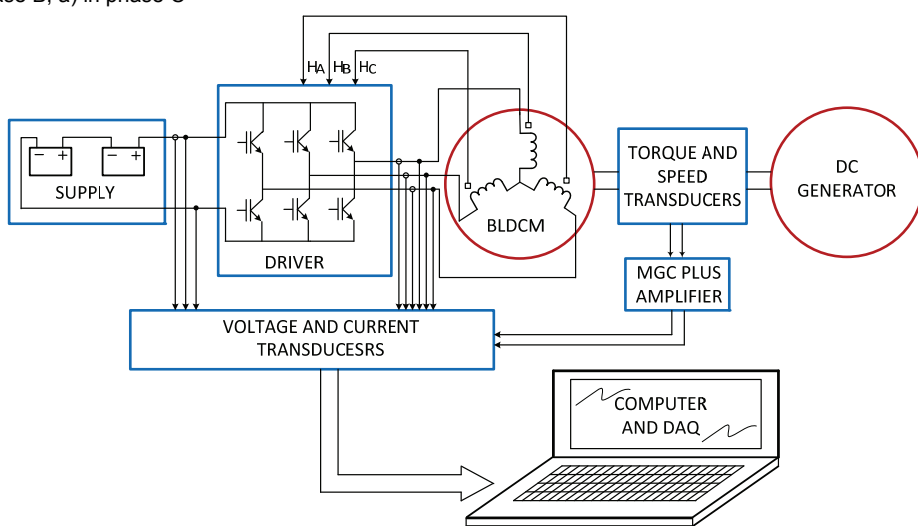


Fig. 16. Block diagram of the measurement set for investigations of the brushless direct current motor

The measurement set contains the following units:

- the brushless DC motor with permanent magnet under investigation,
- direct-current generator rated $P_N = 1.3$ kW. The generator and adjustable value resistor are the load of the BLDCM motor,
- non-contact transducer T32FNA used to measure torque and rotational speed, by Hottinger Baldwin Messtechnik company,
- special clutches connecting transducer T32FNA with examined BLDCM motor and the load. Those clutches eliminate shaft height differences,
- MGCPlus amplifier co-operating with the above-mentioned transducer T32FNA,
- computer with software and 12B multifunction DAQ device, with which it is possible to record voltages and currents, torque and rotational speed,
- accumulators and microprocessor inverter making it possible to adjust the rotational speed and moment. Rotor positions signals are conducted to the above-mentioned inverter,
- a set of Hall transducers adapted to measure voltages and currents, torque and rotational speed.

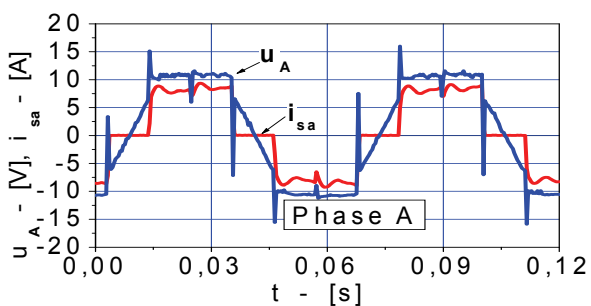
The technique of measuring voltages, current, torque and rotational speed with the use of Hall – transducers and torque transducers, which do not produce the effect of measured signals transfer from the bearings of brushless motor, eliminates problems with measurement signals separation.

The most important features of the driver based on Allegro MicroSystems Inc. A3933SEQ microcontroller are as follows:

- supply voltage ranging 12–28 V,
- bipolar supply to three-phase windings of brushless DC motors,
- over – current protection,
- the control of the electronic commutator built of six MOSFET transistors, on the basis of signals from rotor position sensors (Hall sensors),
- dynamic braking of controlled brushless motor,
- rotation direction control,
- smooth adjustment of rotational speed,
- under-voltage protection and damage indication.

Registered waveforms in steady-state of phase currents (the red waveforms) and voltages (the blue waveforms) for the examined brushless DC motor in the individual phases of windings when the mechanical torque is equal to 10 Nm are presented in Fig. 17, Fig. 18 and Fig. 19.

a)



b)

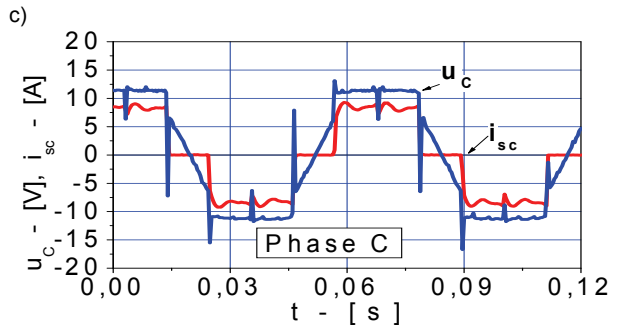
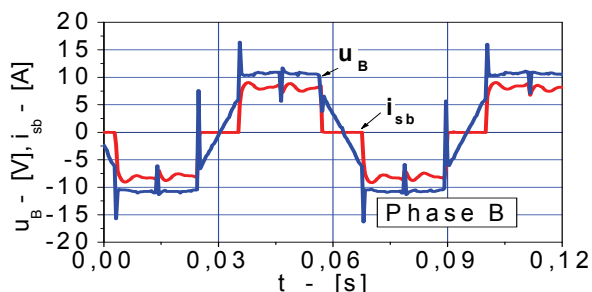


Fig. 17. Steady-state waveforms of phase voltages and currents
a) in phase A, b) in phase B, c) in phase C

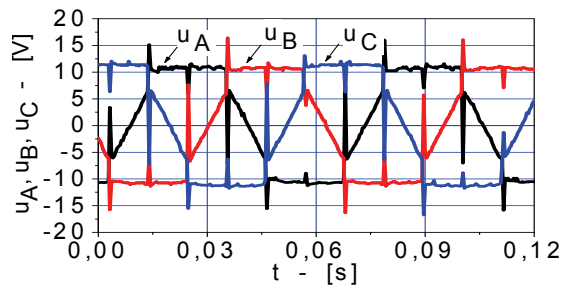


Fig. 18. Steady-state waveforms of phase voltages

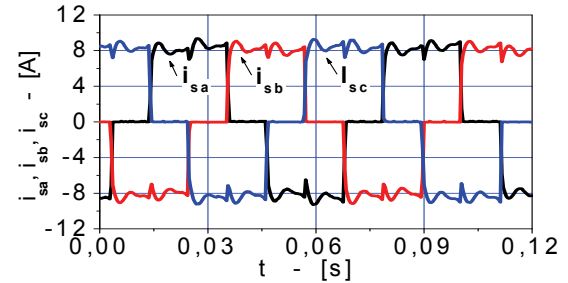


Fig. 19. Steady-state waveforms of armature currents

Fig. 20 shows the electromagnetic torque that was computed with the use of expression $T_e = \frac{e_A i_{s,a}}{\Omega} + \frac{e_B i_{s,b}}{\Omega} + \frac{e_C i_{s,c}}{\Omega}$ on the grounds of registered

waveforms of voltages and currents (Fig. 13) and the output torque T . Measurements were taken at rotational speed 116.4 rpm and average value of output torque $T_{AV} = 10\text{Nm}$.

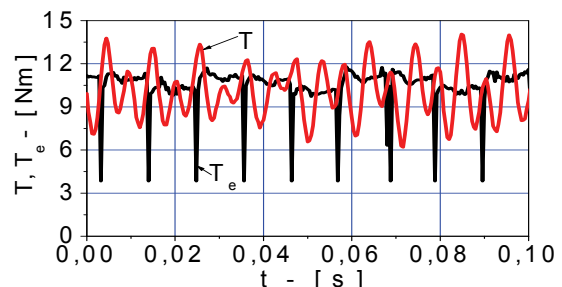


Fig. 20. Waveforms of electromagnetic torque and output torque

Waveforms of output torque and electromagnetic torque shown in Fig. 18 demonstrate the difference between instantaneous values of output torque and electromagnetic torque. Therefore, output torque cannot be presented exclusively as moment T_E , received by means of computation as it is not the case in reality and can lead to serious mistakes. BLDCM motors generate torque pulsation, which results from the stepped change in the angle between the axis of the resultant flow of armature winding and the axis of excitation flux. It seems reasonable, therefore to change the fashion of control of the BLDCM motors, by means of, e.g. appropriate control

of electronic commutator. It can be carried out through the so-called over-commutation [2]. The problem is still investigated by the research team and the results will be presented in papers, which will follow later on.

Conclusion

The paper presents simulation studies in Matlab/Simulink of the steady-state waveforms of phase voltages and armature currents in phase A, in phase B and in phase C and electromagnetic torque of the brushless direct current motor with permanent magnets with three-phase winding connected in star, rated data $P_N=125W$, $U_N=24V$ and $\Omega_N=120\text{rpm}$. The brushless direct current motor, discussed in the paper, constitutes a driving element and it was built in the front wheel hub of the electric bike. On the basis of simulations brushless direct current motor generate torque pulsation, which results from the stepped change in the angle between the axis of the resultant flow of armature windings and the axis of excitation flux. It seems reasonable, therefore to change the way of BLDCM control, by means of, e.g. appropriate control of electronic commutator. The problem of torque pulsation not only in BLDCM but in Permanent Magnet Synchronous Motor and Switch Reluctance Motor is still investigated by the research team and the results will be presented in papers, which will follow later on. In the paper waveforms of simulation and registered steady states of electrical and mechanical quantities: voltages, currents and electromechanical torque for the mechatronic drive system (two accumulators connected in series, the control system of the electronic commutator built of six transistors, the investigated BLDCM and its direct-current generator as the load of the BLDCM) in a test-bed especially designed and constructed for the experiment have been carried out.

Moreover, experimental investigations of the impulse electric circuit for transferring the energy to accumulators coming from induced electromotive forces in BLDCM windings in the electric bike leading to increase the bike travelling distance (about 10 – 15%) were presented. Extending the battery working time depends on the shape of the road and the frequency of charging batteries while

driving. Utilization of the impulse electric circuit of transferring the energy coming from induced electromotive forces allows the driver on optimum choice between the travelling speed smooth regulation and the value of battery charging current. In the paper the induced electromotive forces in three-phases of investigated BLDCM and armature currents, battery charging currents and battery charging voltages versus motor speed and voltage duty-cycle of the switching transistors were shown.

REFERENCES

- [1] Ciurys M., Dudzikowski I.: Analiza parametrów elektro-mechanicznych rozrusznika samochodowego z silnikiem bezszczotkowym. Prace Naukowe IMNiPE, Politechniki Wrocławskiej, Nr 60 2007.
- [2] Dudzikowski, I., Pawalczyk, L.: Permanent magnet DC motors and their control. Actual state and prospects for development, Zeszyty Naukowe Politechniki Śląskiej, Gliwice 2001. Poland.
- [3] Frydlewicz A., Szumińska U., Żochowski K., Krasucki J., Rostkowski A.: Zastosowanie silników bezszczotkowych (BLDC Motor) w napędach hybrydowych. Przegląd elektrotechniczny Nr 12, 2009.
- [4] Hendershot J.R., Miller T.J.E.: Design of brushless permanent magnet motors. Magna physics publishing and Clarendon Press. Oxford 1994
- [5] Nadolski R., Gawęcki Z., Staszak J. Ludwinek K.: Gearless drive of light electric vehicles on the example of the bicycle driven with brushless DC motor with three-phase winding, 4th International Workshop on Research and Education in Mechatronics 2003, October 2003, Bochum, Germany.
- [6] Wiak S., Nadolski R., Ludwinek K., Gawęcki Z.: Brushless DC Permanet Magnet Motor for Electric Bike and their Impulse System for Battery Charging, IJEET - International Journal of Electrical Engineering in Transportation, vol. 1, n°1, 2005.

Autors: Prof. Roman Nadolski, DSc Krzysztof Ludwinek, DSc Jan Staszak, DSc Marek Jaśkiewicz, Kielce University of Technology, Al. Tysiąclecia PP. 7, 25–314 Kielce, Poland,
E-mail: r.nadolski@tu.kielce.pl, k.ludwinek@tu.kielce.pl, j.staszak@tu.kielce.pl, m.jaskiewicz@tu.kielce.pl